In-Line Fiber-Optic Near-Infrared Spectroscopy: Monitoring of Rheological Properties in an Extrusion Process. Part I.

M. G. HANSEN, S. VEDULA

Department of Chemical Engineering, 419 Dougherty Building, University of Tennessee, Knoxville, Tennessee 37996–2200

Received 14 November 1996; accepted 8 July 1997

ABSTRACT: In-line monitoring of chemical processes is desired for its numerous advantages, such as lesser waste, lower developmental cycle time, and lesser costs. In this study, a methodology is presented for estimating polymer rheological properties using fiber-optic near-infrared (NIR) spectroscopy. Predictive calibration models are developed for simultaneous, in-line monitoring of polymer melt flow index (MI) and comonomer concentration for a system of poly(ethylene vinyl acetate) copolymers. The NIR spectra of flowing, molten poly(ethylene vinyl acetate) (EVA) copolymers are collected in a flow cell attached to a single-screw extruder. Multivariate statistical regression analysis is presented for correlation of MI and absorbance in the methylene (C—H) stretch, first overtone NIR wavelength region (1620–1840 nm). Results for simultaneous, real-time monitoring of MI and comonomer composition are discussed in detail.
 J Appl Polym Sci 68: 859–872, 1998

Key words: melt flow index; near-infrared spectroscopy; extrusion; copolymer; melt rheology

INTRODUCTION

NIR spectroscopy has numerous advantages, such as remote data collection capabilities coupled with rapid data analysis methods, availability of fiber optics, and lack of sample-handling problems. Consequently, it has proven to be an ideal analytical technique for chemical process monitoring. In-line measurements of chemical composition, polymer relative viscosity, and polymer morphology have been carried out in earlier studies.[1,2] Feasibility studies have been conducted of composition measurements under extreme process conditions, for example, molten flowing polymers during extrusion, with focus on development of fiber optics, optical probes, and near real-time measurements.[3–6] The fiber-optic probes used for this purpose should be robust enough to withstand such conditions, as the probes are mounted directly into the molten flow stream. Because commercial probes with capabilities to endure such harsh conditions have become available, such measurements have been made feasible.[7,8] This technology is now being employed in the commercial industry and is no longer restricted to measurements made using off-line laboratory instrumentation. Attempts are being made to extend the applicability of this technology to estimate industrially important processing parameters, for example, MI and dynamic rheological properties in near real-time.[9]

The following work will demonstrate the feasibility of extending this technique to make simultaneous measurements of polymer MI and composition of molten EVA samples. A procedure will be described using multivariate statistical tools

Correspondence to: M. G. Hansen.
Journal of Applied Polymer Science, Vol. 68, 859–872 (1998)
 CCC 0021-8995/98/060859-14

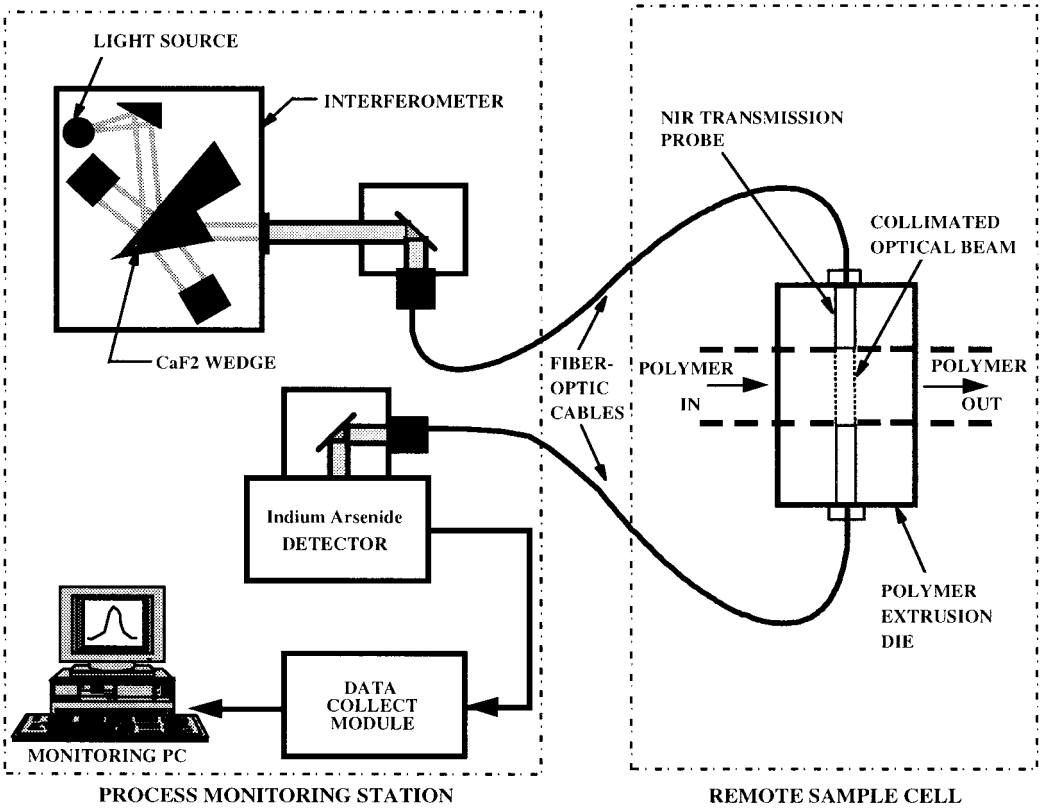

Figure 1 Schematic of the experimental setup for in-line Fourier transform near-infrared spectrometry of molten, flowing polymers.

for developing calibration models, which will be utilized for real-time estimation of rheological properties during extrusion.

THEORY

Correlation of Rheological Properties with NIR Absorption Spectra

In this work, in-line NIR measurements were carried out on molten, EVA copolymers in an extrusion process. During polymer extrusion, the rheological flow behavior of molten polymers is anisotropic. The extent of anisotropic nature of flow is governed by the level of molecular orientation and the orientation distribution of flowing polymer melt. Under nominal extrusion operating conditions involving more or less constant shear rates, these anisotropic effects will be strong functions of polymer weight-averaged molecular weight ($\bar{M}_w$), MWD, chain length, entanglements, and branching parameters. It is expected that these varying levels of orientation and orientation distribution in the optical measurement volume would affect the NIR absorption spectra in some manner. These rheological effects on the NIR spectra, which are attributed to anisotropic rheological flow, are lower order magnitude effects.

In the NIR absorption spectra, variations in chemical composition are dominant effects, and in this study, these variations of comonomer concentration are termed as the primary factors of variation. Compared to the strong, primary effects of chemical composition, the rheological flow effects are only subtle variations in the NIR spectra, and these lower order variations are termed as secondary factors of variation. It is noted that these rheological effects contain important information about physical properties that directly correlate with the molecular weight parameters. One such industrially important parameter is the polymer MI. In a very generic sense, MI is inversely related to the polymer molecular weight parameters, such as the $\bar{M}_w$ values.[10] At moderately low stress values, the MI resembles an "in-

Table I Laboratory Measurements for Comonomer Concentration and MI Values in EVA Samples

Sample Number	VA Concentration (wt %)	Melt Index (g/10 min)
1	0	1.89
2	9.08	6.45
3	12.12	7.79
4	12.04	0.34
5	15.18	7.84
6	17.91	0.64
7	18.06	6.92
8	24.89	17.54
9	25.22	370.0
10	28.49	6.07
11	27.84	143.0
12	28.59	368.0
13	28.37	23.68
14	32.05	37.8

verse" viscosity, and a high MI value implies a low zero-shear viscosity, η_o, or a low $\bar{M}_w$ value. In general, for EVA random copolymers, these rheological properties are not related to the comonomer ratio of ethylene and vinyl acetate (VA). Only at very high VA concentrations (>30 wt % VA), the incorporation of VA favors increased branching in the copolymer, and subsequently, affects rheological behavior to some extent.[11]

Therefore, the primary effects (due to chemical composition) and secondary effects (due to rheological flow) on the absorption spectra are independent; and these effects can be separated to provide simultaneous information about the chemical composition and rheological functions. In the following sections, the experimental studies will be described, and results will be detailed for quantitative analysis of the MI-absorbance relationship.

APPARATUS

Figure 1 shows a schematic of the system for inline molten polymer analysis used in this study. Molten polymer is produced by a 3/4-inch Brabender single screw extruder, with an L/D ratio of 25:1. The polymer from the extruder is pumped to a gear pump. A uniform mass flow rate of the polymer is supplied from the gear pump to a variable pathlength flow cell. For the rectangular flow channel in the flow cell, the nominal shear rate was estimated at $\sim 25\ s^{-1}$. All EVA samples were extruded at more or less constant shear rates. A temperature gradient is maintained in the extruder to produce homogeneous melting and proper conveying of the polymer along the screw. The temperature of the flow cell at the exit port of the gear pump was set at 200°C. This is the temperature at which the NIR spectra were collected. The temperature and pressure conditions are regulated by a temperature and pressure control unit. Dual transmission fiber-optic probes commercialized by Sensotron Inc.™ are used to transmit light through the polymer flow stream.[7] Details of the fiber-optic probe development have been reported in an earlier work.[12] The optical path length in the flow cell, or the distance between the probe windows, is varied by using mechanical spacers of different dimensions. In the current setup, the path length can be varied between 1 and 9.5 mm. A path length of 2.5 mm was used for the current set of experiments. This path length was chosen to keep the maximum absorbance at less than 1.0. A 1.5-mm diameter optical beam is produced by the Sensotron™ NIR transmission probes.

The fiber-optic probes are connected via 500-μ single-fiber fiber-optic cables to an Analect™ Diamond-20 (DS-20) Fourier transform near-infrared spectrometer (FT-NIR).[13] This spectrometer is equipped with an interferometer that works on the moving-wedge principle. For measurements in the NIR region of the electromagnetic spectrum, the wedges are made up of calcium fluoride (CaF_2). The spectrometer uses a quartz halogen lamp as the source and an Indium Arsenide (InAs) detector with CaF_2 windows. The wavenumber resolution used for the current experiments is $8\ cm^{-1}$.

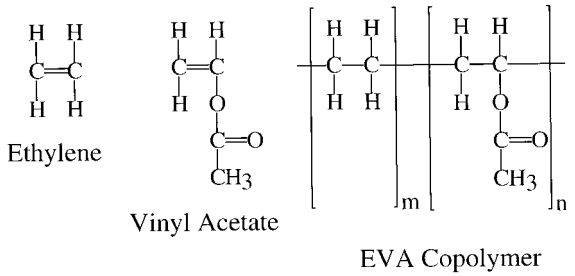

Figure 2 Chemical structure of ethylene and vinyl acetate monomers and poly(ethylene vinyl acetate) (EVA) copolymer.

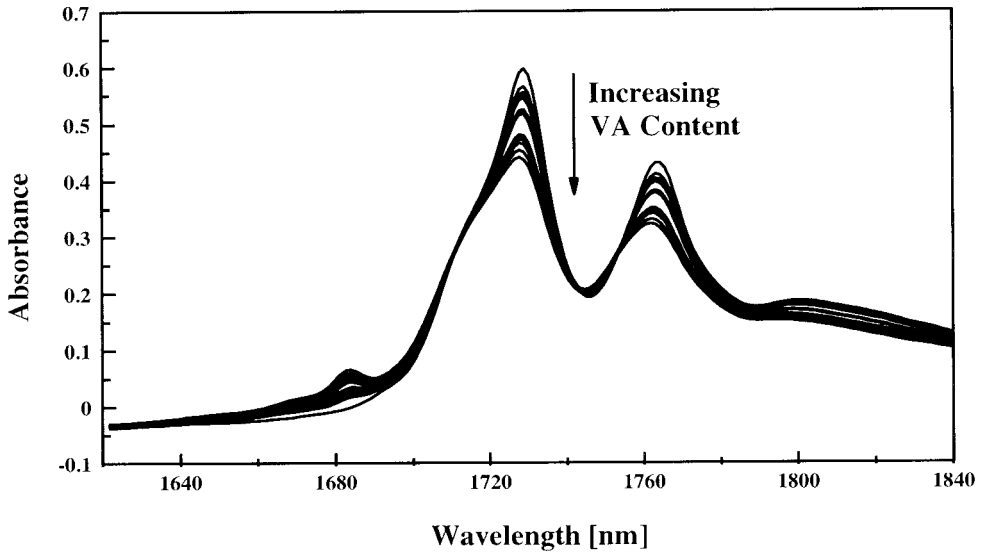

Figure 3 Overlaid absorbance spectra of EVA samples in the NIR wavelength region of 1620–1840 nm. The absorbance band is attributed to methylene (C—H) stretch, first overtone vibrational mode.

EXPERIMENTAL

The system of EVA samples chosen for this study consisted of primarily two factors of variation, namely the comonomer ratio or the concentration of VA in the copolymer, and $\bar{M}_w$. The $\bar{M}_w$, combined with the branching in the polymer, governs the melt viscosity of the polymer through the extruder die. In this context, the melt index is related to both the $\bar{M}_w$ and the branching in the polymer chains. Table I shows the VA content and MI values for the available EVA samples. It is observed that the VA concentration varies from 0 wt % to 32 wt %, and the MI values vary from 0.34 g/10 min to 370 g/10 min. The primary analysis for the melt index values was carried out using ASTM standardized analysis procedure and equipment[13] at the laboratory facility of the company that provided the samples.

The in-line NIR transmission spectra of EVA samples were collected in the melt, in the wavelength range of 1000 to 2500 nm. Ten replicate spectra were collected for each sample, and each spectrum was averaged over 64 scans. Figure 2 shows the chemical structures of the monomers and the EVA copolymer. Figure 3 shows a plot of the overlaid absorbance spectra of EVA samples in the NIR wavelength range of 1620 to 1840 nm. The absorbance band in this wavelength region corresponds to the first overtone vibrational mode of methylene (C—H) stretching,[14] and is a common feature for all macromolecules. (Note the presence of methylene in EVA copolymers in Fig. 2.) With the incorporation of VA into the copolymer, the number density of the C—H stretch vibrations in the optical measurement volume (2.5 mm long and 1.5 mm in diameter) decreases. This leads to a decrease in the intensity of the polyethylene doublet around 1725 nm and 1765 nm. This difference in the absorbance values allows for the quantification of VA. Subtle changes are observed in the shoulders of the methylene stretch doublet. A second region (not shown in Fig. 3), tentatively assigned to a combination band of carbonyl (C=O) and C—H stretches, occurs in the wavelength range 2000 to 2200 nm, with a peak at 2135 nm. This peak increases with an increase in the VA content.

ANALYSIS

Mathematical

In attempts to correlate the MI with the absorbance spectra, it was observed that the range of MI values in the available set was very large. Samples were available with a wide range of MI values, from very high viscosity (MI $\sim$ 0.34 g/10 min) to very low viscosity (MI $\sim$ 370 g/10 min).

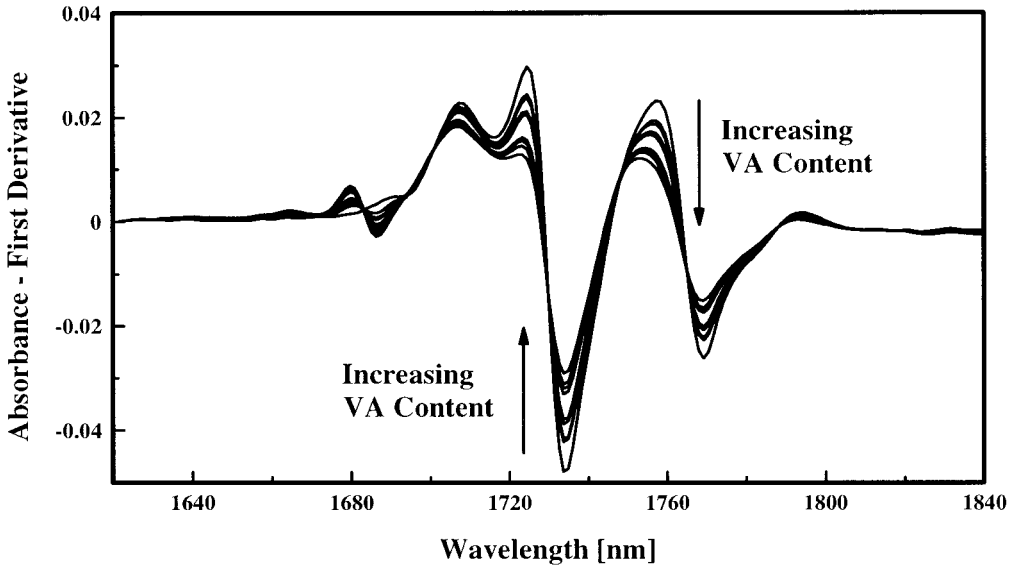

Figure 4 Overlaid plot of absorbance-first derivative spectra of EVA samples in the NIR wavelength region of 1620–1840 nm. The absorbance band is attributed to methylene (C—H) stretch, first overtone vibrational mode. Differentiated spectra are free of baseline offsets and provide better spectral resolution.

This implies that there is significant variation in the $\bar{M}_w$ parameters among the samples. Because such large variations lead to only subtle effects of lower order magnitude on the NIR spectra, it is assumed that a first-order response from the $\bar{M}_w$ paramaters absorbance relationship can be obtained by expressing the xx parameters in terms of their natural logarithms. Such data preprocessing also amounts to "linearizing" the variables used for regression. Therefore, in conjunction with the above assumption, any rheological parameter, such as MI, must be processed before regression using the same correlation of natural logarithms. The theoretical justification for using natural logarithms for such rheological properties comes from the definition of material functions, for example zero-shear viscosity in dynamic rheological experiments. For polymer melts with molecular weights greater than the critical molecular weight M_c, the zero-shear viscosity is given by the proportionality:

$$\eta_o \propto \bar{M}_w^a \qquad (1)$$

where η_o is the zero-shear viscosity, and a is a constant exponent. Berry and Fox[15] observed that for linear homopolymers of narrow molecular weight distribution, $a = 3.4$. The above expression implies that the relationship of $\bar{M}_w$ with most rheological material functions is nonlinear. Taking the natural logarithm of the expression on both sides, the following "affine" relationship is obtained:

$$\ln(\eta_o) = \ln(K) + a \ln(\bar{M}_w) \qquad (2)$$

where K is a constant of proportionality. In the previous section, it was mentioned that the MI variation with $\bar{M}w$ parameters and η_o was of an inverse proportionality. This relationship could be expressed as follows:

$$\ln(\mathrm{MI}) \propto -k \ln(\eta_o) \qquad (3)$$

Therefore, in the multivariate data analysis for melt index, the **Y** matrix consists of ln(MI) values. Linearity is retained by mean-centering the **Y** columns, such that the ln(K) term vanishes after subtraction.

Multivariate Analysis

The absorbance peaks in the NIR spectra are broad and cover a large wavelength range. Unlike the narrow, sharp peaks in the mid-IR region that correspond to fundamental vibrational bands, the NIR region consists of first and higher overtones

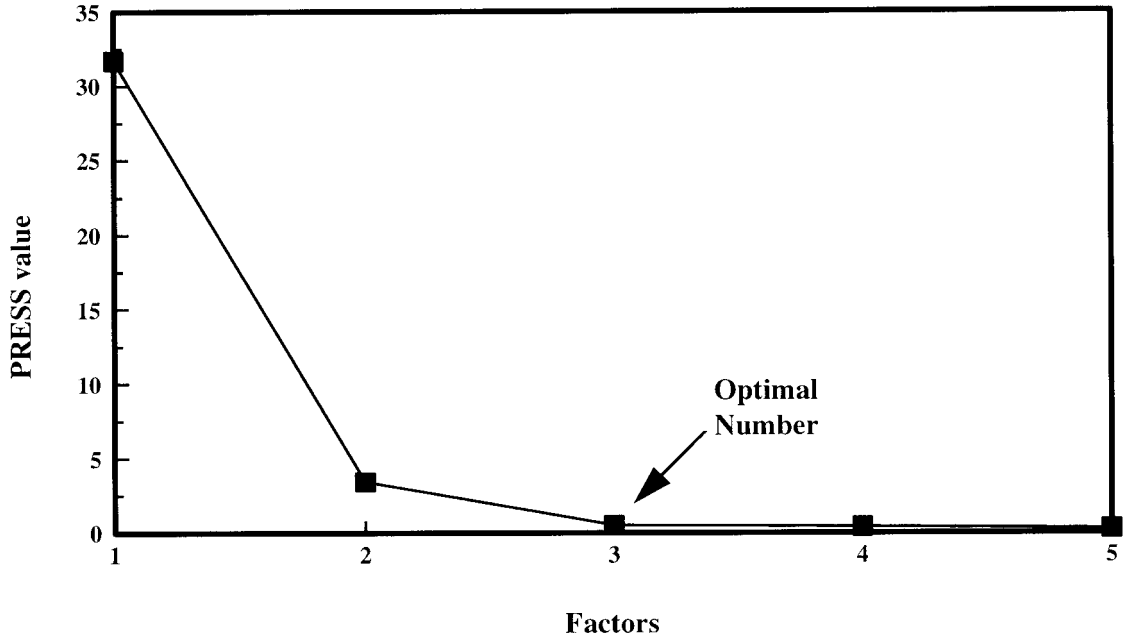

Figure 5 PLS calibration of ln(MI): PRESS plot for five factors obtained from LAS crossvalidation. The optimal number of factors was chosen using the PRESS criterion coupled with an *F*-statistic criterion.

of these fundamental bands. Therefore, the NIR regime comprises of broader bands and considerable band overlap, unlike the mid-IR region. This makes quantitative analysis more difficult and simple multiple linear regression (MLR) techniques cannot be used.[16] Mathematical modeling for NIR spectra requires multivariate techniques such as partial least squares (PLS) and principal component regression (PCR).[17–20] These methods involve data reduction of these highly correlated spectra into a few factors that explain much of the variance in the data. The current work used PLS for data analysis and details of PCR, and its differences from PLS can be found in ref. (17).

In both methods, it is assumed that the property being calibrated, **Y** (e.g., VA concentration, melt index, etc.) can be obtained from the absorbance spectra, **X**. In PLS, both **X** and **Y** matrices are used for data compression. While building a calibration model for the data sets using PLS, the first few factors (also called principal components, or latent variables, or eigenvectors) that explain much of the variance in the covariance matrix, $\mathbf{X}^T\mathbf{Y}$, are evaluated, where $\mathbf{X}^T$ is the transpose of **X**. Details of this procedure are given in ref. (17). The latent variables can be rejected because they explain small variances, usually just random noise in the data. A qualitative interpretation often results in relating the initial principal components directly to the original variables. Thus, PLS is a very powerful tool for both quantitative and qualitative analyses, and helps in the formation of robust calibration models.

A calibration model that uses an optimal number of factors is desired. Using fewer factors in the calibration model would mean excluding important information from the model, and using more factors would imply including noise and thus, higher residuals in the predictions. Therefore, the choice of an optimal calibration model with minimum residuals is critical. Several statistical terms are introduced that help determining the optimal number of factors. These terms are described below[2]:

1) PRESS (Predicted Residual Sum of Squares) value

$$\text{PRESS}_j = \sum_{i=1}^{N} (y_i - \hat{y}_{i,j})^2 \qquad (4)$$

where $\hat{y}_i$ and y_i are the predicted and actual property values respectively, of the i-th sample. N is the number of samples used for calibration, and

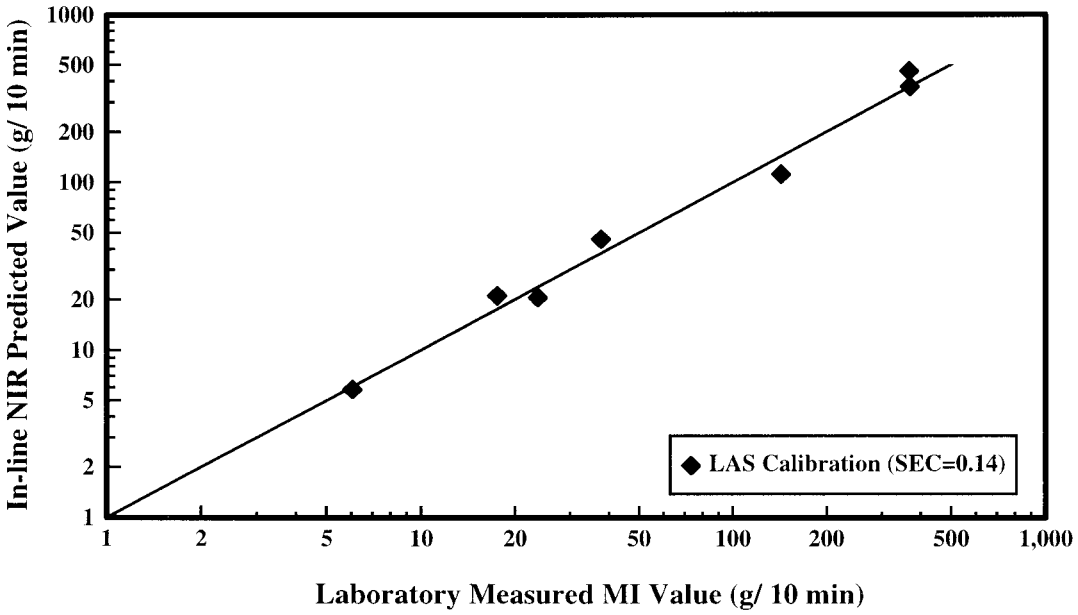

Figure 6 LAS crossvalidation results: MI predictions for samples in the calibration set. In this figure, it is observed that the NIR predicted MI values show excellent agreement with the laboratory measured MI values.

j is an index for the number of latent variables incorporated into the model. The PRESS value is a measure of the residual error, and the optimal number of factors is decided by a minimum PRESS value criterion.

2) SEC (Standard Error of Calibration)

$$\mathrm{SEC} = \sqrt{\frac{\sum_{i=1}^{\mathrm{NC}} (y_{i,c} - \hat{y}_{i,c})^2}{\mathrm{NC} - 1}} \qquad (5)$$

where $\hat{y}_{i,c}$ and $y_{i,c}$ are the predicted and the actual property values of the i-th sample in the calibration set, respectively. NC is the number of samples used in the calibration set.

After the calibration model is developed, it is used to predict the desired property of interest, $\mathbf{Y}$ of an independent test set (also called the prediction set). A residual error term, the standard deviation between the laboratory value and the predicted value (calibration model), is defined for these predictions, as follows:

3) SEP (Standard Error of Prediction

$$\mathrm{SEP} = \sqrt{\frac{\sum_{i=1}^{\mathrm{NP}} (y_{i,p} - \hat{y}_{i,p})^2}{\mathrm{NP}}} \qquad (6)$$

where $\hat{y}_{i,p}$ and $y_{i,p}$ are the predicted and the actual property values of the i-th sample in the prediction set, respectively. NP is the number of samples in an independent prediction set.

RESULTS AND DISCUSSION

To separate the lower order, secondary rheological effects from the strong, primary features of chemical composition in the NIR spectra, it was essential to choose a random sample set for calibration, where the two variables of VA content and ln(MI) values had low correlation in their numerical entries. Therefore, care was taken to avoid inadvertently capturing any information about VA content, while developing a calibration model for ln(MI). In this context, a statistical term called the correlation coefficient, r, is introduced, which is defined as follows:[16]

$$r = \frac{\mathrm{cov}(\mathbf{x}, \mathbf{y})}{\sqrt{\mathrm{var}(\mathbf{x})\mathrm{var}(\mathbf{y})}} \qquad (7)$$

where for any given variables $\mathbf{x}$ (e.g., VA content) and $\mathbf{y}$ (e.g., MI), var($\mathbf{x}$) and var($\mathbf{y}$) are the vari-

Table II Total y-Block Variance Explained for Different Factors

Number of Factors Retained	VA Calibration Model Total *y*-Block Variance Explained (%)	MI Calibration Model Total *y*-Block Variance Explained (%)
1	99.7	36.5
2	99.9	95.6
3	99.9	99.6

ances of $\mathbf{x}$ and $\mathbf{y}$, respectively, and cov($\mathbf{x}$, $\mathbf{y}$) is the covariance of $\mathbf{x}$ and $\mathbf{y}$.

An r value close to 1.0 implies very high correlation between the two variables, while an r value close to 0 implies that the distribution of the two variables is random. To obtain a strict random distribution, a very large sample set is required. Unfortunately, such a large sample set is rarely commercially manufactured, and only a limited set of 14 samples was available for analysis. Therefore, from the available sample set, a subset of sample spectra was chosen for which the VA concentration values and ln(MI) values had very low correlation, to develop a trial calibration model for ln(MI). A successful MI-calibration for this sample subset would mean that the melt index is an independent physical factor of variation, which is inherent in the absorbance spectra of these samples. Because the MI and VA content variations were random for this subset, it would ensure that a "false" relationship is not extracted between the two variables due to numerical collinearity.

For the trial subset, EVA samples were selected in the VA content range of 24 wt % VA to 32 wt % VA and ln(MI) values in the range of 1.8 (MI ~ 6 g/10 min) to 6 (MI ~ 370 g/10 min). In effect, while developing the trial model, large VA variations were suppressed, and significant variations in the MI values were incorporated. The correlation coefficient was a low value of 0.10 for the trial set, which implied a fairly random set.

Once a successful relationship between the ln(MI) values and the absorbance spectra was established using the trial calibration model, a new calibration model will be developed with an enlarged sample set. This sample set will include a wide range of variation in both VA content (wt % VA ~ 0 to 32) and ln(MI) values (ln(MI) ~ 0.34 to 6). The final calibration model will be tested for MI predictions of EVA samples belonging to two categories: (1) EVA samples with similar MI values but widely varying VA content, and (2) EVA samples with widely varying MI values but similar VA composition. A detailed analysis

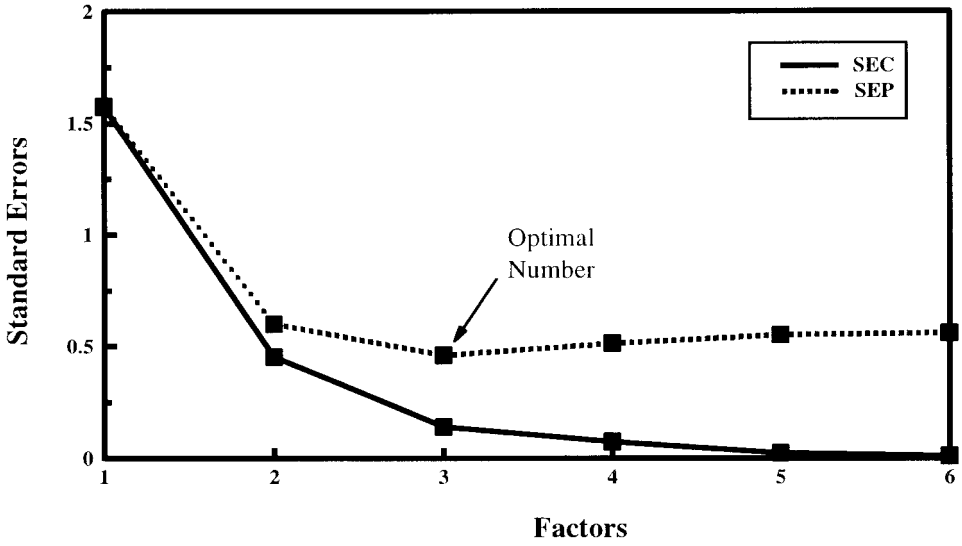

Figure 7 Standard errors plot for PLS models with different principal components. As expected, the SEC curve shows a decreasing trend with increasing number of factors. The optimal number of factors is decided by the minimum PRESS value and an *F*-statistic criterion.

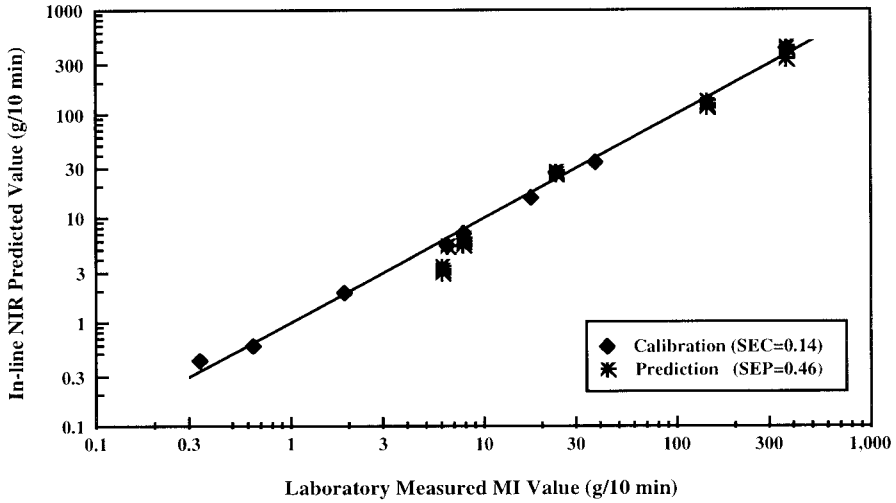

Figure 8 Plot illustrating the NIR predictions for melt index, MI. The MI calibration model was built using ln(MI) values. A three-factor model was used for optimal predictions for ln(MI) using the PRESS and the *F*-statistic criteria.

of the development of both the trial and the final calibration models is given below.

Ten replicate spectra for each sample were included in the analysis. First derivatives of the spectra were taken to build the trial calibration model. Differentiated spectra (Fig. 4 are free of any baseline offsets and expose any subtle variations in the spectra, although they are noisier. The smoothed data were standardized by mean-centering as a part of pretreatment. Mean-centering involves subtracting the mean of each column in the **X** and **Y** matrices from the data points. One spectrum, the average of the 10 replicate spectra, for each sample in the subset was included to form the calibration set.

For the MI trial calibration model, the **Y** matrix consisted of one column, of size $(m \times 1)$, with the ln(MI) values corresponding to each sample. A PLS model based on the singular value decomposition (SVD) method was utilized for evaluating the principal components.[20] The calibration model was developed by using a crossvalidation technique, called the leave-a-sample (LAS) approach.[2] The LAS crossvalidation procedure was essential because the sample set was not large enough for two separate calibration and prediction subsets. According to this approach, one sample was left out from the calibration model every time and chosen as an internal validation set. This sample was predicted from a calibration model developed on the remaining samples. Several such calibration models were developed, with additional principal components being incorporated each time. The residual errors for the predictions of this excluded sample were evaluated from the actual values and the NIR predicted values, as a function of the number of principal components. In the next step, this sample was included into the calibration set and another sample was removed; and a similar procedure was followed. This process was continued until all samples in the original calibration set were left out from the calibration at least once and used for internal validation. The crossvalidation procedure is also advantageous in that it highlights sample outliers. Outlier samples are those samples that do not fall in the linearity range decided by the calibration model, and these are identified by unusually large prediction errors, or PRESS values. If there are far too many outliers, it means the existence of either a nonlinear relationship or lack of any relationship between **Y** and **X**.

The optimal number of principal components, or factors, was decided by evaluating a cumulative PRESS term. For every principal component, this term was calculated by summing the individual PRESS values for each sample [according to eq. (4)]. The number of factors retained in the final calibration model corresponded to a minimum cumulative PRESS value. In addition to the PRESS value, an *F*-statistic criterion was used to decide the optimal number of principal components required for calibration.[19] This criterion is a statistical method, which takes into account the relative

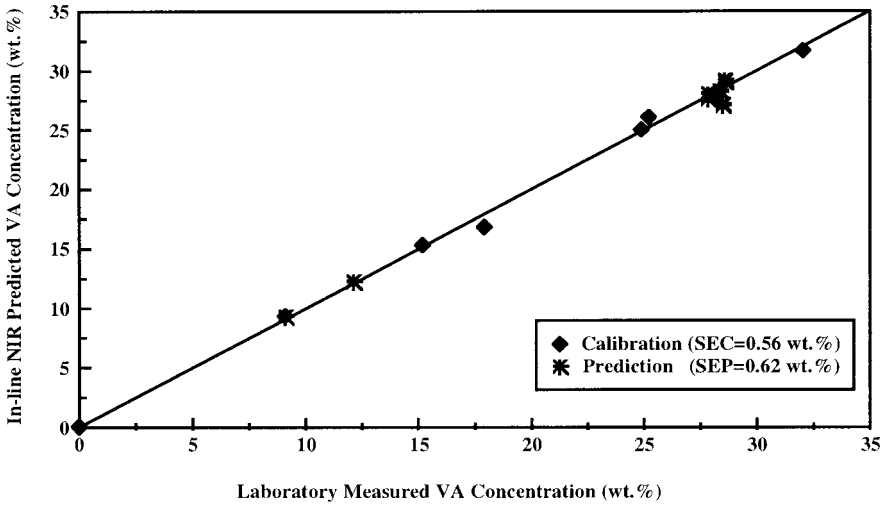

Figure 9 Plot illustrating the NIR predictions for vinyl acetate, VA concentration (wt %). A one-factor model was developed for predicting the VA content using the PRESS and the *F*-statistic criteria.

importance of incorporating additional factors into the calibration model.

The cumulative PRESS plot vs. number of principal components is illustrated in Figure 5. In combination with the *F*-statistic criterion, this plot suggested a model with three factors for optimal MI predictions. Using eq. (5), the standard residual error for the model, or the SEC value, was found to be 0.14 (on a natural log scale). Figure 6 shows the predictions for samples in the calibration set, with a calibration model based on three factors. This plot shows excellent agreement for the NIR predictions of MI with the actual MI values obtained from primary analysis.

The above trial model established that there is independent information about the rheological response in NIR absorbance spectra. With suitable data preprocessing in the form of natural logarithms, multivariate techniques can be used to correlate physical properties, such as MI with the absorption spectra. With the success of the trial model, the sample set was enlarged to include larger variations in both variables, namely the VA content and the MI values. This sample set was used to develop the final calibration model that would be used for real-time monitoring during polymer extrusion.

In conjunction with the MI calibration model, a separate independent calibration model was developed to predict the VA concentration. Because the VA content is a strong, dominant feature in the absorbance spectra, it is expected that a one-component principal component would be sufficient to estimate VA concentration.[3] This result was corroborated using the PRESS and the *F*-statistic criteria. Because the rheological flow effects are secondary effects, a larger number of principal components are expected for optimal predictions. From the earlier results on the trial calibration set, a three-factor model was developed for predicting ln(MI). Table II shows the variance explained in the **Y**-blocks for the two calibration models. From this table, it is observed that three factors are required to explain about 99.6% variance in the MI data, while only one factor is sufficient to account for about 99.7% variance in VA content. For MI calibration, the inclusion of a second principal component explains an additional variance of 59.1%. Hence, the second principal component is most significant during MI calibration and contains maximum information about MI variance.

An external prediction set was formed using spectra of samples, which were not included in the calibration set. The calibration models developed above were used to predict the samples in the prediction set. The SEP values, as evaluated from eq. (6), for the two models were 0.46 for MI predictions (three-factor model) and 0.62 wt % for VA predictions (one-factor model). A plot of the standard errors in the calibration and prediction set for the MI-calibration model is shown in Figure 7. In this

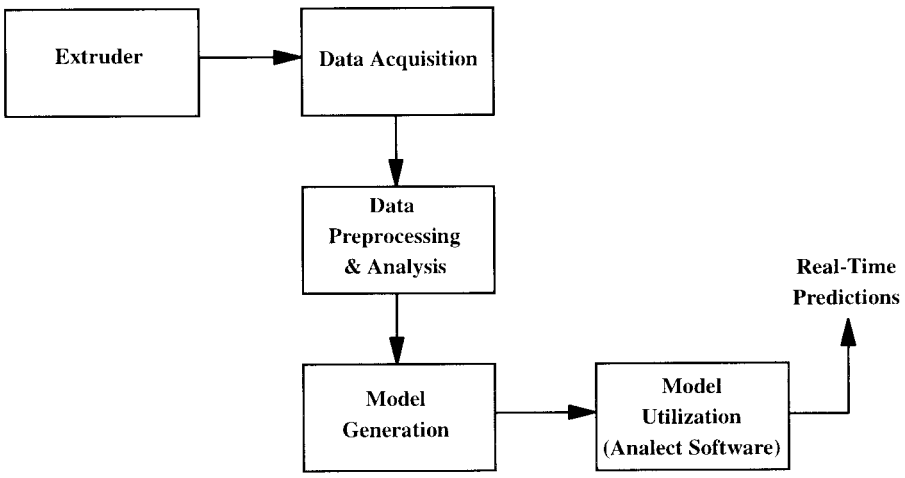

Figure 10 Schematic for real-time monitoring of VA content and melt index in EVA copolymers.

figure, the SEP curve reiterates the fact that three principal components give minimum residual error for MI. The in-line predictions for ln(MI) and VA concentration for the final calibration and prediction sets are shown in Figures 8 and 9, respectively. Excellent agreement is observed between the actual, laboratory primary analysis and the in-line, NIR predicted MI and VA values.

Real-time Predictions during In-Line Extrusion

Finally, the stability of the predictions using the calibration models was tested for simultaneous, real-time predictions of MI and VA concentration during extrusion. A generic schematic of the methodology for real-time monitoring is presented in Figure 10. EVA samples were continuously fed through the extruder, and test scans were taken. Data preprocessing of these spectra (such as first-derivative, mean-centering, etc.) was carried out in a similar manner to the sample spectra used for calibration. Each spectrum was averaged over 16 scans and every fifth spectrum was saved. One spectrum was saved after approximately every 40 s. The two calibration models built earlier were then used to estimate the desired properties of VA content and MI. The real-time process monitoring modules, PC80™ and FSP6802B,™ available in the Analect™ calibration software, were used for spectral data collection during extrusion.[8]

The stability of predictions of the calibration models were tested on six EVA samples belonging to two different classes were used for real-time predictions. Class A consisted of EVA samples with widely varying VA concentrations, but similar MI values. These constituted the first three samples in Table III. Four EVA samples were included in Class B. These samples consisted of $\sim$ 28 wt % VA and had very different MI values. The samples in the two classes (one sample overlaps in the two classes), were continuously fed through the extruder in the order in which they are presented in the table.

The real-time predictions for VA content and MI for Class A and Class B samples are illustrated in Figure 11. It is observed that most predictions lie within the limits set by the SEP values. This implies that the predictions for both VA concentration and ln(MI) lie between the actual laboratory value $\pm$ SEP. (In the figure, these limits are defined as the upper and lower detection limits, UDL and LDL, respectively.) It is demonstrated that the calibration

Table III EVA Samples for Real-Time Monitoring

Sample Number	Class Identity	VA Concentration (wt %)	ln(MI) Values
1	A	9.11	1.86
2	A	12.12	2.05
3	A & B	28.49	1.80
4	B	27.84	5.91
5	B	28.59	4.96
6	B	28.37	3.16

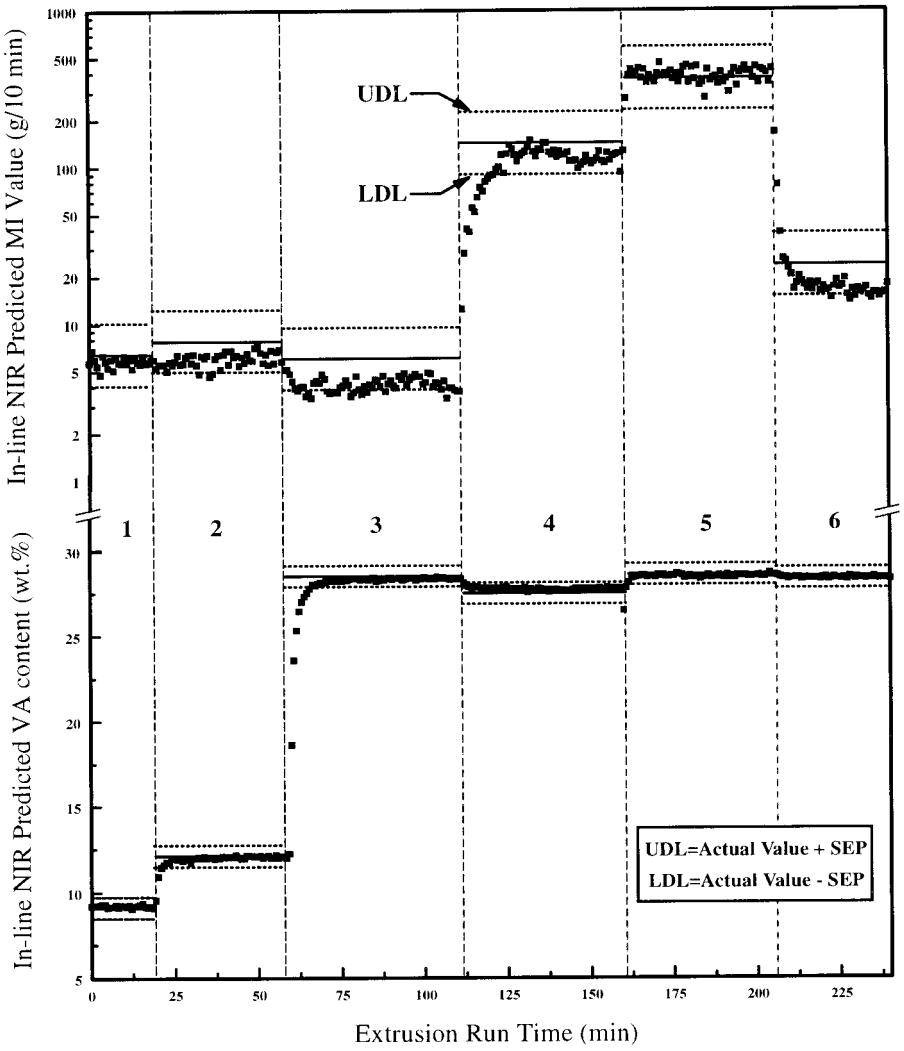

Figure 11 In-line, real-time predictions for MI and VA content in Class A (samples numbered 1, 2, and 3) and Class B (samples numbered 3, 4, 5, and 6) EVA samples. The predictions for both primary (VA content) and secondary (MI) variables lie within SEP limits associated with the calibration models. (SEP for VA-calibration model = 0.62 wt %; SEP for MI-calibration model = 0.46 on a natural log scale.) The transition region between successive samples exhibits intermediate properties of VA content and MI. This region is also an indicator of the average sample residence time in the extruder. (UDL: upper detection limit; LDL: lower detection limit.)

models can successfully estimate samples belonging to both classes. This reiterates that the PLS calibration models can separate the two independent factors of variation in the EVA samples, namely MI and VA concentration.

Another observation is made in the smooth transition region between any two successive samples. In this region, a "blend" of the two samples is expected in terms of both VA content and melt viscosity conditions. This "blend" would progressively change in both VA composition and MI from the previous sample to the new sample. In Figure 11, it is observed that the calibration models capture the expected behavior in the transition region with regard to intermediate properties of VA content and melt viscosity in the blend. The transition region is also an indicator of the average residence time of the sample in the extruder, gear pump, and flow

cell. According to the figure, the MI values seem to take a longer time to stabilize to steady values than the VA concentration values.

CONCLUSIONS

During extrusion of molten polymer melts, anisotropic effects associated with the rheological flow translate into variations in the NIR absorption spectra. These effects allow correlation of rheological properties, such as polymer MI with the NIR spectra. In this study, a methodology is demonstrated for simultaneous in-line monitoring of both VA content and MI values in molten EVA copolymers. It is established that the variation of MI in EVA copolymers is independently observed in the NIR absorption spectra. The robustness of calibration models was tested by real-time predictions on EVA samples belonging to two categories: (1) EVA samples with similar MI values but widely varying VA content, and (2) EVA samples with widely varying MI values but similar VA composition. The ability of the models to estimate samples in these two distinct groups further validated the robustness of calibration. The predictions for both VA concentration and MI lie within detection limits decided by the SEP limits (0.62 wt % and 0.46, respectively).

In the above experiments, one disadvantage is the use of isotropic light. Unlike polarized light spectrometry, which allows a more detailed understanding of the mechanisms involved in molecular orientation during flow (information in the form of flow birefringence and dichroism), the rheological flow effects observed in isotropic spectroscopy experiments are small, and at best, can be observed only in higher order factors. Therefore, powerful mathematical tools, such as multivariate techniques, have to be used for data analysis and model development.

NOMENCLATURE

Symbol	Abbreviation	Description
η_o		Zero-shear viscosity, [Pa.s]
a		Berry-Fox exponent
c		Used as a subscript to denote sample in calibration set
EVA		Ethylene-vinyl acetate copolymer
j		Array
K		Proportionality constant
k		Array
LAS		Leave-a-sample cross-validation approach
LDL		Lower detection limit for quantification
MI		Melt flow index, [g/10 min]
$\bar{M}_w$		Weight average molecular weight of the polymer, [g/mol]
MWD		Molecular weight distribution in the polymer
m		Index, number of rows in a matrix
NC		Number of samples in calibration set
NIR		Near-infrared
PCR		Principal component regression
PLS		Partial least squares
PRESS		Predicted residual sum of squares
p		Used as a subscript to denote sample in prediction set
r		Correlation coefficient
SEC		Standard error of calibration
SEP		Standard error of prediction
SVD		Singular value decomposition of a matrix
T		Used as a superscript to denote transpose of a matrix
UDL		Upper detection limit for quantification
VA		Vinyl acetate comonomer, in EVA copolymer
$\mathbf{X}$		NIR absorbance data matrix
$\mathbf{x}$		Vector
$\mathbf{Y}$		Rheology data matrix
$\mathbf{y}$		Vector
y		Regressed variable
$\hat{}$		Symbol used to denote estimated values of variables, obtained from regression

REFERENCES

1. M. P. B. van Uum, H. Lammers, and J. P. de Kleijn, *Macromol. Chem. Phys.,* **196,** 2023 (1995).
2. C. E. Miller, Ph.D. dissertation, University of Washington, Seattle (1989).
3. A. Khettry, Ph.D. dissertation, University of Tennessee, Knoxville (1995).
4. W. M. Doyle, *Process Control Qual.,* **2,** 11 (1992).
5. M. P. B. van Uum, H. Lammers, and J. P. de Kleijn, *Macromol. Chem. Phys.,* **196,** 2029 (1995).
6. H. L. McPeters and S. O. Williams, *Process Control Qual.,* **3,** 75 (1992).
7. Sensotron, Inc., 5881 Engineer Drive, Huntington Beach, CA 92649.
8. Axiom Analytical, Inc., 18103 Sky Park South, Unit C, Irvine, CA 92714.

9. D. Marrow, paper 459 presented at Pittsburgh Conference on Analytical Chemistry and Applied Spectroscopy, Chicago (March 1996).
10. J. D. Ferry in *Viscoelastic Properties of Polymers,* John Wiley & Sons, Inc., New York (1980).
11. J. Edenbaum, in *Plastics Additives and Modifiers Handbook,* Chapman and Hall, New York (1996).
12. M. G. Hansen and A. Khettry, *Polym. Eng. Sci.,* **34,** 1758 (1994).
13. ASTM Standards, D1238, vol. 08.01 (1986).
14. R. F. Goddu, *Adv. Anal. Chem. Instrument.,* **1,** 347 (1960).
15. G. C. Berry and T. G. Fox, *Adv. Polym. Sci.,* **5,** 261 (1968).
16. J. O. Rawlings, *Applied Regression Analysis: A Research Tool,* Wadsworth & Brooks, Pacific Grove, CA, 1988.
17. H. Martens and T. Naes in *Multivariate Calibration,* John Wiley and Sons Ltd., New York, 1989.
18. A. Hoskuldsson, *J. Chemometr.,* **9,** 91 (1995).
19. D. M. Haaland and E. V. Thomas, *Anal. Chem.,* **60,** 1193 (1988).
20. T. W. Wang, A. Khettry, M. Berry, and J. Batra, The First International Chemometrics Internet Conference, INCINC '94, Sept.–Nov., 1994)